JOURNAL OF AGRICULTURAL AND FOOD CHEMISTRY

Protective Effect of Ginseng on Cytokine-Induced Apoptosis in Pancreatic β-Cells

HYE YOUNG KIM* AND KYONG KIM

Food Function Research Division, Korea Food Research Institute, San 46-1 Baekhyun-dong, Bundang-gu, Songnam-si, Kyonggi-do 463-746, Republic of Korea

The effects of ginseng extracts (GE) and several ginsenosides on cytokine-induced apoptosis were evaluated. In pancreatic β-cell line MIN6N8 cells, the inhibitory effect of GE was significantly observed at 25−100 μg/mL: an 86−100% decrease of cytoplasmic DNA fragments quantified by an ELISA. The inhibitory effect of red ginseng (RG) extract was greater than that of white ginseng (WG) extract (IC_{50}, 3.633 vs 4.942 μg/mL). Screening of several known ginsenosides, which were present in ginseng extracts at 0.124−1.19% (w/w) by HPLC analysis, revealed that the ginsenosides were responsible for the inhibition of β-cell apoptosis at 0.1−1.0 μg/mL. The molecular mechanism, by which GE inhibited β-cell apoptosis, appeared to involve the reduction of nitric oxide (NO) and reactive oxygen species (ROS) production, inhibition on p53/p21 expression, and inhibition on cleavage of caspases and poly-(ADP-ribose) polymerase (PARP). This study suggests that ginseng may inhibit cytokine-induced apoptosis in β-cells and, thus, may contribute via this action to the antidiabetic influence in type 1 diabetes.

KEYWORDS: Ginseng; cytokines; apoptosis; pancreatic β-cells; diabetes

INTRODUCTION

The roots of ginseng have been used to treat diabetes (*1*). Results of type 1 (*2*−*5*) and type 2 (*5*−*8*) animal studies and clinical trials (*9*−*11*) support the claim that ginseng possesses antidiabetic function. However, the components and mechanisms responsible for its antidiabetic action have yet been unknown.

Apoptosis, programmed cell death, is probably the main form of β-cell death in both type 1 and type 2 diabetes. In type 1 diabetes, β-cell destruction is believed to be mediated by inflammatory cytokines such as interleukin (IL)-1β, interferon (IFN)-γ, and tumor necrosis factor (TNF)-α produced by auto-aggressive T lymphocytes. In type 2 diabetes, progressive β-cell loss may be mediated by high concentrations of circulating free fatty acids and glucose, because these have been demonstrated to induce β-cell apoptosis in vitro (*12*).

Cytokines induce apoptosis through the concerted action of a number of intracellular signaling pathways in β-cells, including the generation of nitric oxide (NO) and reactive oxygen species (ROS), loss of mitochondrial transmembrane potential ($\Delta\psi m$), and induction of p53 and p21, c-jun NH_2-terminal kinase/stress-activated protein kinase (JNK/SAPK) activation, Bax oligomerization, cytochrome *c* release, proteolytic cleavage of procaspases, and poly(ADP-ribose) polymerase (PARP) (*13*).

To elucidate the mechanisms by which ginseng exerts antidiabetic action in type 1 diabetes, we tested the hypothesis that ginseng could protect β-cells against apoptosis induced by cytokines. Attempts were also made to compare the relative potency of two kinds of ginseng, that is, red ginseng (RG, *Ginseng Radix Rubra*, steam-treated white ginseng) and white ginseng (WG, *Panax ginseng* C. A. Meyer). White ginseng is air-dried ginseng, and red ginseng is produced by steaming raw ginseng at 98−100 °C for 2−3 h (*1*). Red ginseng is reported to have more bioactivity than the no-processed white ginseng roots (*1*).

The constituents found in most ginseng species included ginsenosides, polysaccharides, peptides, polyacetylenic alcohols, and fatty acids (*1*). Many of the medicinal effects of ginseng are attributed to the triterpene glycosides known as ginsenosides (ginseng saponins) (*1*, *14*). Up to now, more than 80 ginsenosides have been isolated from ginseng, and most of them exhibit four types of aglycone moieties: protopanaxadiol, protopanaxatriol, ocotillol, and oleanolic acid. The difference between protopanaxadiol (PPD)-type ginsenosides and protopanaxitriol (PPT)-type ginsenosides is the number of hydroxyl moieties. We further tested whether saponins found in the extract, the seven ginsenosides (**Figure 1**), could account for the observed effect of ginseng extract. To explain the anti-apoptotic mechanism of ginseng, we focused the effects of ginseng on generation of NO and ROS, induction of p53/p21, and the cleaved activation of caspase-3, -7, and -9 and PARP in cytokine-treated β-cells.

MATERIALS AND METHODS

Ginseng. RG roots were purchased in dried forms from Korea Ginseng Corp. (Daejeon, Korea). WG roots were purchased in dried forms from Gae-sung Ginseng Corp. (Kyunggido, Korea). Both kinds of ginseng were *Panax ginseng*-strained, 6-year-old, cultivated in Korea,

* Author to whom correspondence should be addressed [telephone 82-31-780-9267; fax 82-31-709-9876; e-mail khyey@kfri.re.kr].

10.1021/jf062577r CCC: $37.00
Published on Web 03/24/2007

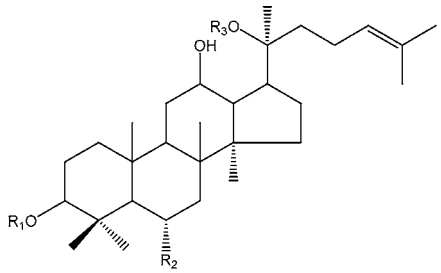

Ginsenosides	R_1	R_2	R_3
Rb_1	Glc-^{2}Glc-	H	Glc-^{6}Glc-
Rb_2	Glc-^{2}Glc-	H	Ara(pyr)-^{6}Glc-
Rc	Glc-^{2}Glc-	H	Ara(fur)-^{6}Glc-
Rd	Glc-^{2}Glc-	H	Glc-
Re	H	Rha-^{2}Glc-O-	Glc-
Rf	H	Glc-^{2}Glc-O-	H
Rg_1	H	Glc-O-	Glc-

Figure 1. Structures of the ginsenosides. Abbreviations for carbohydrates are as follows: Glc, glucopyranoside; Ara (pyr), arabinopyranoside; Ara (fur), arabinofuranoside; Rha, rhamnopyranoside.

and straight-shaped in dried forms. The dried weight of one root was 20 g. Ginsenosides Rb_1, Rb_2, Rc, Rd, Re, Rf, and Rg_1 were purchased from Extrasynthese (Genay, France).

Preparation of Ginseng Extracts. Each ginseng product was ground to pass an 80 mesh sieve and extracted under reflux with ethanol:water (80:20, v/v) at a material-to-solvent ratio of 20 mL/g for 2 h, followed by filtration with filter papers (Toyo Advantec No. 2 and 4, Toyo Roshi Kaisha, Ltd., Japan), and then, the process including the addition of solvent, extraction under reflux and filtration was repeated three times. The combined filtrate was concentrated with a rotary vacuum evaporator at 40 °C until all extraction solvent was completely removed so that solid residue was obtained. The yield was 33% for RG and 27% for WG, by weight, of the original ginseng powder. The residue was dissolved in dimethyl sulfoxide (DMSO) and used for subsequent bioassays. The final concentration of DMSO in cell incubation medium never exceeded 0.1%, which we determined did not affect apoptosis in preliminary experiments (unpublished observations).

Analysis of Ginsenosides in the Extracts. An Agilent 1100 liquid chromatograph (Waldbronn, Germany) equipped with quaternary gradient pump, autosampler, and diode array detector was used. A Waters Symmetry C_{18} reversed-phase column (150 × 3.9 mm, i.d., 5 μm, Waters Corp., Milford, MA) was used. The mobile phase consisted of water (solvent A) and acetonitrile (solvent B). The gradient elution was used as follows: 0−20 min, 20% B; 25 min 30% B; 35 min, 40% B; 45−50 min, 100% B; 55 min, 20% B. The column temperature was kept constant at 35 °C, and the flow rate was 1 mL/min (*15*).

Cell Lines and Reagents. MIN6N8 cells, SV40 T-transformed insulinnoma cells derived from nonobese diabetic (NOD) mice, were kindly provided by Prof. Myung-Shik Lee (Sungkyunkwan University School of Medicine, Seoul, Korea) under the permission of Prof. Junichi Miuagaki, Osaka University, Osaka, Japan (*16*). Cells were grown in Dulbecco's modified Eagle's medium (DMEM) containing 15% fetal bovine serum (FBS), 2 mmol/L glutamine, 100 IU/mL penicillin, and 100 μg/mL streptomycin (GIBCO BRL, Grand Island, NY). Reagents were obtained from the following sources: High glucose DMEM, FBS, trypsin-EDTA 100 IU/mL, penicillin, and 100 ug/mL streptomycin were from Gibco Ltd. (Paisley, Strathclyde, UK). Sodium carbonate and β-mercaptoethanol were from Sigma (St. Louis, MO), and recombinant mouse and *E. coli* derived IL-1β, IFN-γ, and TNF-α were from R&D systems (Minneapolis, MN). The antibodies against polyclonal cleaved caspase-3, -7, -9 and cleaved PARP were purchased from Cell Signaling Technology (Beverly, MA). The antibodies against PARP, p21, p53, and β-actin, were purchased from Santa Cruz Biotechnology Inc. (Santa Cruz, CA). Secondary antibodies were obtained from Vector Laboratories (Burlingame, CA); horseradish peroxidase-conjugated anti goat or anti rabbit, exposed to an enhanced chemiluminescence (ECL) detection system (Amersham Pharmacia Biotech, Piscataway, NJ), and electrophoresis equipment were from Bio-Rad Laboratories (Richmond, CA).

Proinflammatory Cytokine Exposure. Cytokine-mediated apoptosis was induced by incubation with a cytokine mixture of 10 ng/mL each of recombinant mouse IL-1β, IFN-γ, and TNF-α for 0−48 h. The choice of cytokine concentrations and exposure time was based on preliminary experiments. Test reagents (GE and ginsenosides) were added simultaneously with cytokines.

Cell Survival Assay. Cell viability was determined by the reduction of yellow 3-(4,5-dimethylthaizol-2-yl)-2,5-diphenyl tetrazolium bromide (MTT; Sigma Chemical Co.) into a purple formazane product by mitochondrial dehydrogenase of metabolically active cells. Briefly, cells were seeded at a density of 2×10^6 cells/well into 96-well plate. After overnight growth, cells were treated with cytokines and a series of concentrations of GE for 24 h. The final concentrations of DMSO in the culture medium were <0.1%. At the end of treatment, 30 μL of MTT was added, and cells were incubated for a further 4 h. Cell viability was obtained by scanning with an Enzyme-Linked Immunosorbent Assay (ELISA) reader with a 570 nm filter (*17*).

Measurement of DNA Fragmentation. For quantitative determination of apoptotic DNA fragmentation, cytoplasmic histone-associated DNA fragments were measured with the Cell Death Detection ELISA Plus Kit from Roche (Mannheim, Germany) according to the manufacturer's instructions. This assay is based on a quantitative sandwich enzyme immunoassay principle, using mouse monoclonal antibodies directed against DNA and histones. This allows the specific determination of mono- and oligonuclisosomes but not free histone or DNA that may generate during nonapoptotic cell death (*18*) in the cytoplasmic fraction of cell lysates. At the end of the culture period, cells were washed with phosphate-buffered saline (PBS), lysed according to the manufacturer's protocol, centrifuged (200*g*, 10 min), placed in a streptoavidin-coated microtiter plate, and incubated with a mixture of antihistone (biotin-labeled) and anti-DNA (conjugated with peroxidase) antibodies. After removal of the unbound antibodies by a washing step, the amount of nucleosomes was quantified photometrically by the peroxidase retained in the immunocomplex.

Measurement of Nitrite Concentration. Nitrite concentration in the culture supernatant, as a reflection on NO production, was measured using a colorimetric assay (*19*). Cells (2.0×10^5) were cultured in cytokines with various concentrations of GE for 24 h. NO production in medium was measured when aliquots were removed from conditioned medium and incubated with an equal volume of Griess reagent (1% sulfanilamide/0.1% *N*-(1-naphtyl)-ethylenediamine dihydrochloride/ 2.5% H_3PO_4) at room temperature for 10 min. The absorbance at 540 nm was determined using a microplate reader (E-MAX, Molecular Devices, Sunnyvale, CA). Sodium nitrite was used as a standard.

Measurement of Intracellular Peroxide. The intracellular peroxides were estimated using an oxidation-sensitive 2′,7′-dichlorofuorescin diacetate (DCFH-DA; Molecular Probes, Eugene, OR) fluorescent probe. It was reported that the 2′,7′-dichlorofuorescin (DCFH) was oxidized by peroxides in the cell and that DCFH changed to 2′,7′-dichlorofuorescein (DCF) with high fluorescence. The fluorescence of DCF in the cells was estimated using a fluorescense spectrophotometer (*20*).

Preparation of Cell Lysates and Immunoblotting. Cells were collected by centrifugation at 800*g* for 3 min, washed twice with ice-cold PBS, and centrifuged at 800*g* for 3 min. Cells were lysed by suspending the pellet in lysis buffer (cellLytic MT Mammalian Tissue lysis/extraction reagent, Sigma Chemical Co.) for 30 min at 4 °C. The lysates were centrifuged at 13000*g* at 4 °C for 20 min, and the protein contents in the supernatants were measured using an assay kit for protein determination (Quick Start Bradford Dye Reagent; Bio-Rad Lab Inc., Hercules, CA). The supernatant containing 50 μg of protein was separated on 10% SDS-polyacrylamide gels at 20 mA (100 V) and blotted onto immunoblot PVDF membranes (Bio-Rad) in Tris-borate-EDTA buffer. Membranes were incubated for 4 h at room temperature with primary antibody (diluted 1:200−1:1000). In all cases, the excess of primary antibody was removed by three washes with 50 mM Tris−HCl pH 7.5, 150 mM NaCl, 0.1% Tween 20 (TBST); membranes were then incubated with anti-goat or anti-rabbit IgG conjugated with peroxidase (1 μg/mL) for 60 min, and immuno-reactive bands were detected by enhanced chemiluminescence. Immunoblots were analyzed with a GS-800 calibrated densitometer (Bio-Rad).

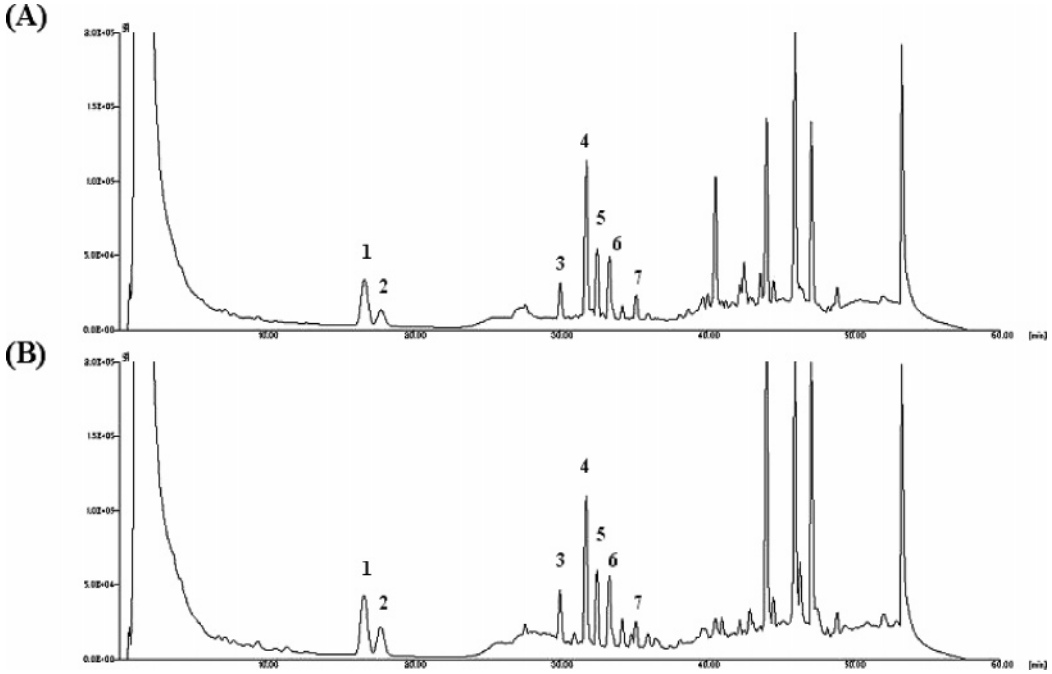

Figure 2. HPLC chromatogram of the extracts of red ginseng (**A**) and white ginseng (**B**) extracts. Peaks: 1, Rg1; 2, Re; 3, Rf; 4, Rb1; 5, Rc; 6, Rb2; 7, Rd.

Statistical Analysis. Experiments were performed in triplicate and replicated three times. All values were expressed as mean and standard deviations (SD) or standard errors of means (SEM). One-way ANOVA followed by Duncan's multiple range test were used for statistical analyses (SAS software, SAS Inc.).

RESULTS

Effect of Ginseng Extracts on Cytokine-Induced Cytotoxicity in MIN6N8 Cells. As a first step, the cytotoxicity of GE on MIN6N8 cells was observed. Each extract of RG and WG was applied in increasing concentrations up to 1000 μg/mL to the cells for 18−48 h. We found that GE in the concentration range 0.1−1000 μg/mL had no cytotoxic effect on the cells, when the cytotoxicity was evaluated by MTT assay (data not shown). Based on this result, each GE was added up to 100 μg/mL. After 24 h of the cytokine treatment, cell viability was determined by MTT assay. As shown in **Figure 3A**, IL-1β or IFN-γ alone did not cause significant cytotoxicity. However, the combined treatment of IL-1β, IFN-γ, and TNF-α decreased the percentage of viable cells to 61.18 ± 7.62% of the cytokine-untreated group. The viability of the cells treated with RG extract (25−100 μg/mL) dose-dependently showed significant protection against the cytotoxicity induced by the cytokines (**Figure 3B**). WG extract (25−100 μg/mL) prevented dose-dependently the cytotoxicity (**Figure 3B**). The result suggests that GE protected against cytokine-mediated cytotoxicity. The inhibitory effect of RG extracts was higher than that of WG extract in the cells (**Figure 3B**).

Effect of Ginseng Extracts on Cytokine-Induced Apoptosis in MIN6N8 Cells. Next, we measured nucleosomal release as an early biochemical feature and quantitative marker of apoptosis (*21*). Incubating MIN6N8 cells with the cytokine combination of IL-1β/IFN-γ/TNF-α resulted in a pronounced stimulation of DNA fragmentation, that is, 25.22 ± 4.22% of untreated control as compared to 67.26 ± 6.29% cytokine-treated (2.7-fold; **Figure 4**). The extract of RG or WG showed no significant influence on nucleosomal release in cytokine-untreated cells (not shown in data). Cytokine-mediated nucleosomal release was significantly inhibited in the presence of RG extract at the concentrations of 25, 50, and 100 μg/mL by 95.5−100% (**Figure 4**). Nucleosomal release was significantly inhibited in the presence of WG extract at the concentrations of 25, 50, and 100 μg/mL by 85.78−98.48% (**Figure 4**). This result suggested that ginseng protected against cytokine-mediated apoptosis. The IC_{50} value of RG extract was 3.633 μg/mL as compared to that of WG extract, 4.952 μg/mL, indicating that RG extract was 1.36 times more effective than WG extract (**Table 1**).

Effects of Ginsenosides on Cytokine-Induced Apoptosis in MIN6N8 Cells. The HPLC profile (**Figure 2**) and content (**Table 2**) of the ginsenosides in each prepared extract was shown. WG shows that typical ginsenoside consists of Re, Rg1, Rb1, Rc, and Rb2. In the case of RG, the contents of polar ginsenosides (peaks 1−3) are slightly decreased, and less polar ginsenosides (peaks 4−7) are increased.

Figure 5 shows the inhibitory activities of ginsenoside Rb1, Rb2, Rc, Rd, Re, Rf, and Rg1, the major saponins of RG and WG, in the cytokine-induced apoptosis. All of the ginsenosides tested significantly and dose-dependently prevented the cytokine-induced apoptosis in the β-cells. The result indicated that the ginsenosides were responsible for the inhibitory activity of GE. The IC_{50} values of the ginsenosides were at the range from 0.07320 to 0.3623 μM (**Table 1**). The order of inhibitory potency among the ginsenosides was Rb2 > Rd > Re > Rg1 > Rb1 > Rf > Rc.

It was noted that the contents of the ginsenosides tested were lower in RG extract than in WG extract and that the panaxadiol (PD)/panaxatriol (PT) ratio was higher in RG extract than in WG extract, whereas the inhibitory effect of RG extract was higher than that of WG extract.

Effect of Ginseng Extracts on Cytokine-Mediated NO Generation. Biologically produced NO is rapidly oxidized to nitrite and nitrate in aqueous solutions (*22*). Nitrite concentration in the supernatant of the culture medium, therefore, represents the NO production. As shown in **Figure 6A**, the incubation of MIN6N8 cells with the cytokines for 24 h revealed an increase

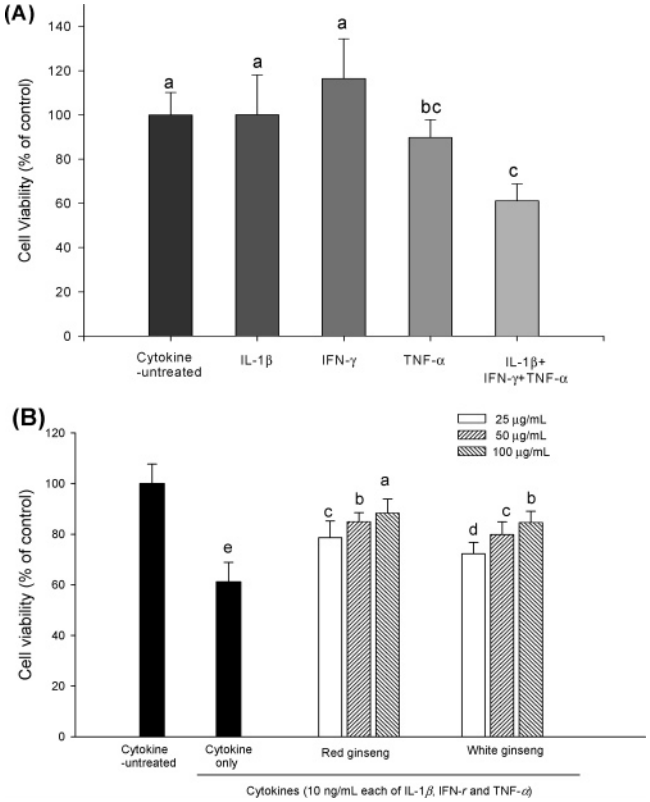

Figure 3. (**A**) Effects of cytokines on cell viability in MIN6N8 cells. The cells (7.0×10^4 cells/well) were treated with IL-1β (10 ng/mL), IFN-γ (200 U/mL, 10 ng/mL), and TNF-α (200 U/mL, 10 ng/mL) or each alone for 24 h. The percentage of cells viable after these treatments was determined by the MTT assay. Values are means ± SEM ($n = 9$) of three independent experiments in triplicates. Means with different letters differ significantly, $p < 0.05$. (**B**) Effects of ginseng extracts on cell viability in cytokine-treated MIN6N8 cells. The cells were treated with three concentrations of the extracts, simultaneously with cytokines for 24 h. The cell viability was determined by MTT assay. Value are means ± SEM, $n = 9$. Means with different letters differ significantly among cytokine-treated groups, $p < 0.05$.

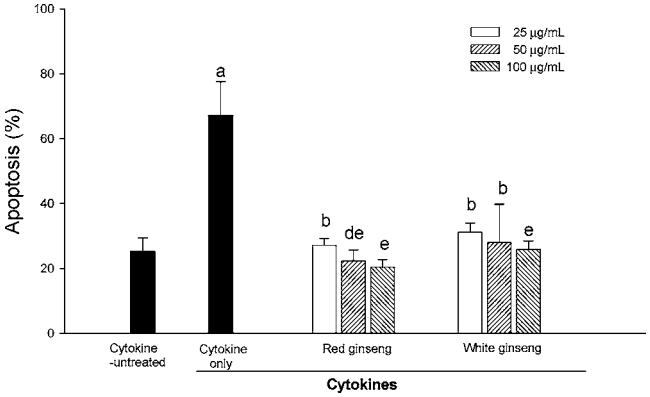

Figure 4. Effects of ginseng extracts on cytokine-induced apoptosis in MIN6N8 cells. The cells were treated with GE and cytokines for 24 h. The amount of cytosolic DNA-associated histone was measured. Values are means ± SEM, $n = 9$. Means with different letters differ significantly among cytokine-treated groups, $p < 0.05$.

of nitrite concentration from 4.67 ± 0.86% of untreated group to 318.2 ± 39.53% of cytokine-treated group (68-fold). Each extract from RG and WG at 25, 50, and 100 μg/mL inhibited nitrite formation dose-dependently (**Figure 6A**). For natural products that could generate nitrite, we checked whether or not

Table 1. Concentration of Ginseng Extracts and Ginsenosides Required To Inhibit 50% of the Control Reaction of Cytokine-Induced Apoptosis in MIN6N8 Cells

samples	IC_{50}[a] μg/mL	IC_{50}[a] μM
red ginseng extract	3.633	
white ginseng extract	4.942	
ginsenosides		
Rb1	0.2540	0.2290
Rb2	0.07900	0.07320
Rc	0.3911	0.3623
Rd	0.07400	0.07813
Re	0.1380	0.1457
Rf	0.1880	0.2347
Rg1	0.1380	0.1723

[a] The concentration of an inhibitor required to inhibit 50% of the control reaction (without inhibitor) under the assay conditions. Calculated from linear regression equation in semilogarithmic manner.

Table 2. Content of Ginsenosides (mg/g Dry Weight of Extract) in the Extract of Red Ginseng and White Ginseng[a]

ginsenosides	red ginseng	white ginseng
Rb1	11.2 ± 0.31 a	10.9 ± 0.06 a
Rb2	4.02 ± 0.13 c	4.66 ± 0.03 bc
Rc	4.10 ± 0.13 c	4.61 ± 0.05 bc
Rd	1.30 ± 0.06 d	1.24 ± 0.15 e
Re	3.52 ± 0.22 c	5.48 ± 0.35 b
Rf	1.45 ± 0.06 d	2.25 ± 0.04 c
Rg1	8.27 ± 0.34 b	11.9 ± 0.28 a
total[b]	33.8	41.0
PD/PT[c]	1.55	1.09

[a] Values are means ± SD, $n = 3$; values within columns having the same letters are not significantly different ($p < 0.05$). [b] Sum of the amount of the seven ginsenosides quantified by HPLC. [c] PD (panaxadiol saponin): sum of Rb1, Rb2, Rc, and Rd. PT (panaxatriol saponin): sum of Re, Rf, and Rg1.

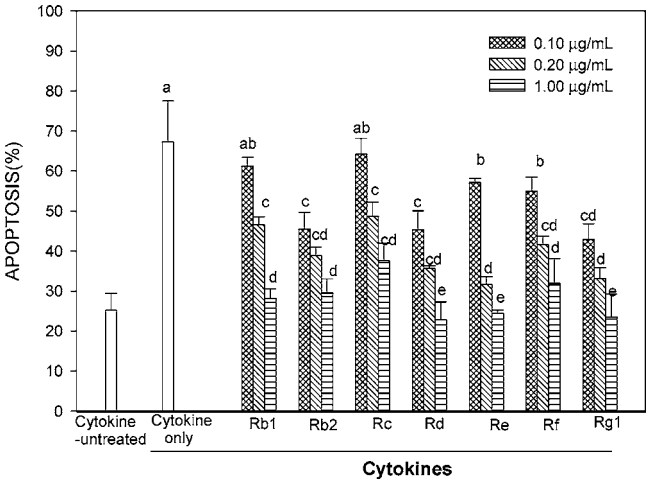

Figure 5. Effects of ginsenosides on cytokine-induced apoptosis in MIN6N8 cells. The cells were treated with ginsenosides and cytokines for 24 h. The amount of cytosolic DNA-associated histone was measured. Value are means ± SEM, $n = 9$. Means with different letters differ significantly among cytokine-treated groups, $p < 0.05$.

GE per se could generate nitrite. Treatment with GE without cytokines did not show any increase of nitrite production (data not shown).

Effects of Ginseng Extracts on Cytokine-Mediated ROS Generation. Intracellular ROS were detected by fluorescein-labeled dye, DCFH-DA. As seen in **Figure 6B**, the cytokine treatment significantly increased the fluorescent intensity of ROS in the cells, that is, 0.45 ± 0.12 mM of untreated control as

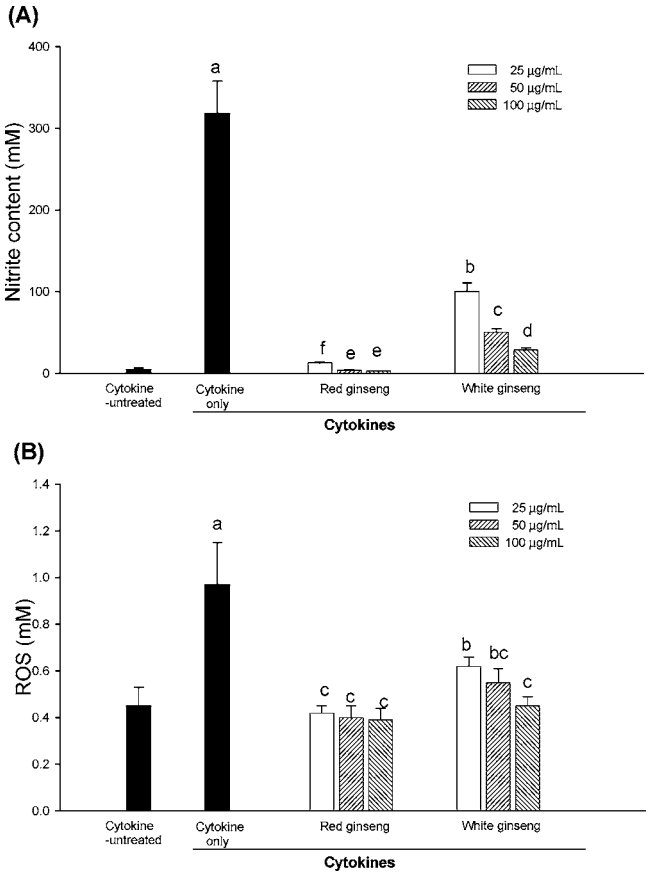

Figure 6. (**A**) Effects of ginseng extracts on cytokine-induced NO production. NO production was determined by measuring nitrite accumulation in the culture medium after 24 h incubation. Values are means ± SEM, $n = 9$. Means with different letters differ significantly among cytokine-treated groups, $p < 0.05$. (**B**) Effects of ginseng extracts cytokine-induced ROS production. ROS production was determined by measuring DCF fluorescence. Values are means ± SEM, $n = 9$. Means with different letters differ significantly among cytokine-treated groups, $p < 0.05$.

compared to 0.97 ± 0.18 mM of cytokine-treated control (2.2-fold). The co-incubation with each extract from RG and WG at 25, 50, and 100 μg/mL for 24 h significantly inhibited the ROS generation (**Figure 6B**).

Effects of Ginseng Extracts on Cytokine-Mediated Activation of Pro-apoptotic Proteins. Among a number of proteins mediated to intracellular signaling pathways to cytokine-induced apoptosis in β-cells, we examined the expressions of caspase-3, caspase-7, caspase-9, PARP, p53, and p21 in cytokine-treated MIN6N8 cells for various time intervals. For the activation of caspase-9, an initiator caspase is necessary for the processing and activation of caspase cascades, and so we examined the cleaved activation of caspase-9. Immunoblot analysis showed that caspase-9 was cleaved 6−48 h after treatment with the cytokines (**Figure 7C**). We next evaluated the processing and activation of caspase-3, which is considered to play a central role in many types of stimuli-induced apoptosis. Caspase-3, one of the effector caspases, was cleaved yielding a 19 kDa fragment for 3−48 h and a 17 kDa fragment for 18−30 h after the cytokine treatment (**Figure 7A**). Caspase-7, another effector caspase, was also cleaved 6−48 h after the cytokine treatment (**Figure 7B**). Our results showed the cleavage of caspase-9, -3, and -7 after the treatment of TNF-α/IFN-γ/IL-1β in MIN6N8 cells. It was reported that cleavage of caspase-3, -7, and -9 occurred after 36 h of TNF-α/IFN-γ treatment of MIN6N8 cells (*23*), and that cleavage of only caspase-3 occurred after 12 h of

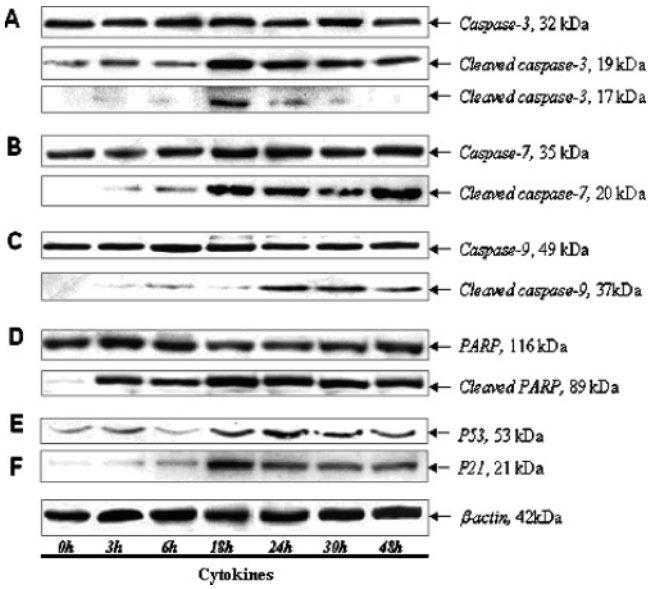

Figure 7. Effects of cytokines on the expression of apoptotic-related proteins, caspase-3 (**A**), caspase-7 (**B**), caspase-9 (**C**), PARP (**D**), p53 (**E**), and p21 (**F**), in MIN6N8 cells. The cells were treated with IL-1β/IFN-γ/TNF-α for different time periods as indicated. Whole cell lysates were separated on SDS-PAGE, followed by immunoblotting. All data are representative of three independent experiments in triplicates. Similar results were obtained for each of the three experiments.

TNF-α/IFN-γ treatment of MIN6N8 cells (*13*). This discrepancy may be due to the presence or absence of IL-1β, and due to differences in the amount and times treated with TNF-α and IFN-γ.

Activation of caspase-3 leads to the cleavage of a number of proteins, one of which is PARP. The cleavage of PARP is the hallmark of apoptosis (*24*). PARP (116 kDa) is cleaved to produce an 89 kDa fragment during apoptosis. Treatment with cytokines caused a proteolytic cleavage of PARP for 3−48 h, time-dependently for 3−18 h with accumulation of the 89 kDa species and concomitant disappearance of the full-size 116 kDa protein (**Figure 7D**), confirming that cytokine-activated caspase-3 was functionally active.

The expression of p53 and p21, well-known potent pro-apoptotic proteins involved in the mitochondrial apoptotic pathway, was also significantly increased for 18−48 h cytokine treatment (**Figure 7E**,**F**). It was reported that p53 protein is a potent transcription factor, activated and accumulated in response to DNA-damage agents, leading to cell cycle arrest or apoptosis (*25*).

The expressions of the pro-apoptotic proteins examined were mostly maximal at 18 h after the treatment of cytokines. Therefore, we evaluated the effects of GE on the expressions of the pro-apoptotic proteins for 18 h treatment of cytokines. The dose-dependent decrease of the cleaved fragment of caspase-9 was observed in RG- or WG-treated cells (**Figure 8C**). The dose-dependent decrease of the cleaved fragment of caspase-3 and -7 was observed in RG- or WG-treated cells (**Figure 8A**,**B**). To examine the cleavage of PARP following the activation of caspase-3, cytokine-treated MIN6N8 cells were treated with or without 25−100 μg/mL of GE for 18 h.

To assess the role of PARP in the anti-apoptotic activity of GE, the expression of PARP was examined by western blot analysis. As shown in **Figure 9A**, the 116 kDa PARP was cleaved to its active 89 kDa in MIN6N8 cells treated with GE.

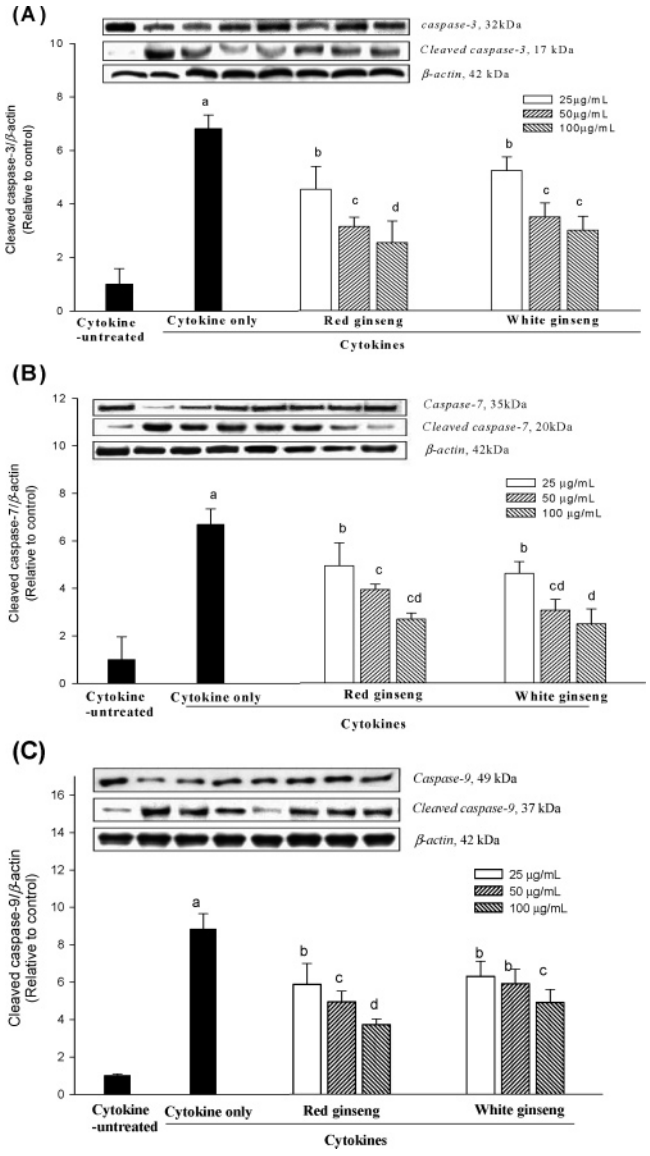

Figure 8. Effect of ginseng extracts on the cleavages of caspase-3 (**A**), -7 (**B**), and -9 (**C**) in cytokine-treated MIN6N8 cells. The cells were treated with cytokines with/without RG/WG extract for 18 h, and western blot analysis was performed. The expressions of cleaved caspases were quantified by densitometric analysis. Data are expressed as the ratio of cleaved caspases to β-actin (means ± SEM, $n = 9$). Means with different letters differ significantly among cytokine-treated groups, $p < 0.05$.

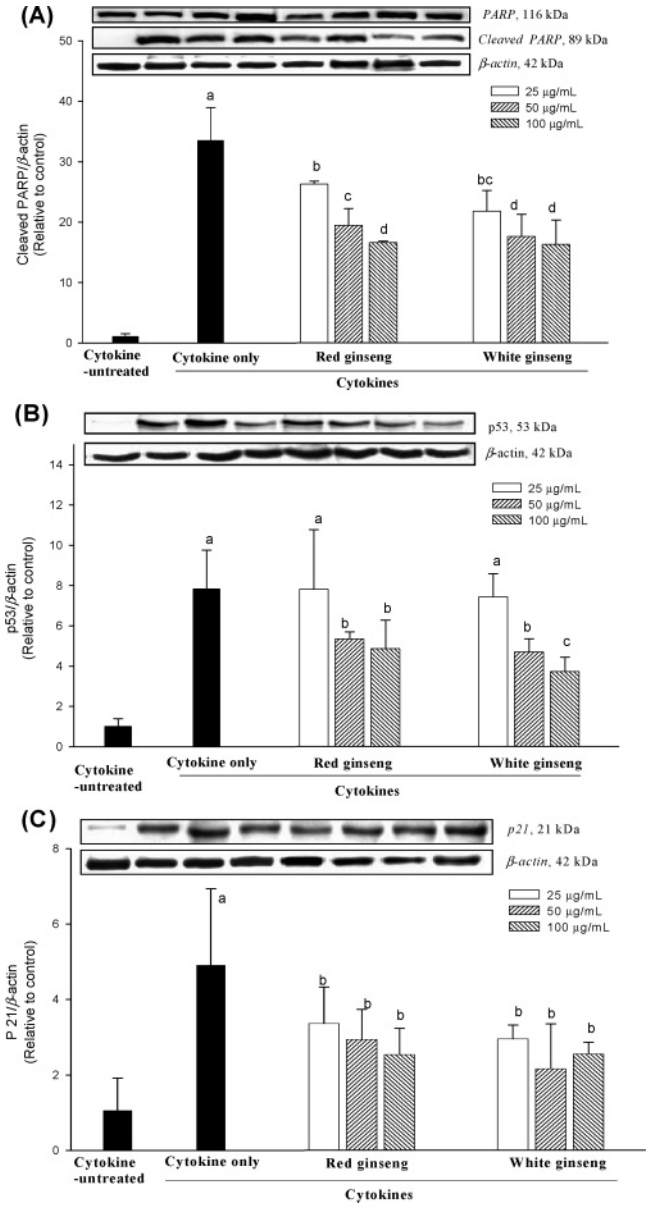

Figure 9. Effects of ginseng extracts on the expressions of cleaved PARP (**A**), p53 (**B**), and p21 (**C**) in cytokine-treated MIN6N8 cells. The cells were treated with cytokines with/without RG/WG extract for 18 h, and western blot analysis was performed. Cleaved PARP, p53, and p21 expression was quantified by densitometric analysis. Data are expressed as the ratio of cleaved PARP, p53, or p21 to β-actin (means ± SEM, $n = 9$). Means with different letters differ significantly among cytokine-treated groups, $p < 0.05$.

To determine the effect of GE on anti-apoptotic pathways, we evaluated transcription factors p53 and p21 expression by western blot. As demonstrated in **Figure 9B**, RG and WG at the concentrations of 50 and 100 μg/mL caused the decrease of p53 expression. As demonstrated in **Figure 9C**, RG and WG at the concentrations of 25, 50, and 100 μg/mL caused the decrease of p21 expression.

DISCUSSION

We demonstrated that GE and several ginsenosides protected MIN6N8 cells from cytokine-induced apoptosis in a dose-dependent manner. This is the first time the anti-apoptotic effect of GE has been demonstrated in cytokine-mediated apoptosis in pancreatic β-cells. The inhibitory effect of RG extract was greater than that of WG extract by 1.36 times on the cytokine-induced apoptosis in MIN6N8 cells. The ginsenosides tested were responsible for the inhibitory activity of GE. However, it might be suggested that the ginsenosides besides the tested ones, or other classes of compounds besides ginsenosides, also contribute to the activity of GE.

Our experimental data showed that GE exhibited inhibitory activity against cytokine-induced generation of NO (**Figure 6A**), which may partly contribute to its anti-apoptotic actions. In pancreatic β-cells, it seems that increased production of NO, due to the induction of NO synthase (iNOS) via the nuclear factor (NF) κB transcription factor, is an important signal in cytokine-induced apoptosis, because inhibition of iNOS has been shown to prevent apoptosis (*26*). It should be further studied that GE could affect the expression of iNOS and NFκB. NO may cause β-cell toxicity via several mechanisms (*27*): (1) NO inactivates the Krebs cycle enzyme aconitase by nitrosulation

of Fe−S group, thereby preventing mitochondrial glucose oxidation and ATP generation; (2) NO damages cellular DNA by causing DNA strand breaks, thereby activating DNA repair mechanisms including PARP, which can cause cell death through depletion of cellular nicotinamide adenine dinucleotide (NAD^+); (3) the NO-induced DNA strand breaks may be sufficient to induce apoptosis through activation of the tumor suppressor protein p53 (*28*); and (4) NO may function as a redox mediator in the cytokine-induced apoptotic pathway. From the result in this study that GE inhibited the expression of p53 in the cytokine-treated cells (**Figure 9B**), the inhibitory activity of GE on NO generation might affect β-cell apoptosis via inhibiting the expression of p53. However, other possibilities should be studied.

The generation of ROS has been believed to be the ultimate cause of cytokine-mediated death in β-cells (*29*). As one of the major sources of ROS, mitochondria are highly susceptible to oxidative damage, causing mutations in mitochondrial DNA and changing $\Delta\psi$m, thereby affecting mitochondrial membrane integrity and preceding cell death induced by cytokines (*30*). The p53 and p21 are critical initiators of the intrinsic apoptosis pathway in response to stress from oncoproteins, DNA damage, hypoxia, and survival factor deprivation (*31*). P53/p21 can also regulate apoptosis by activating mitochondrial genes to enhance ROS generation (*32*) or bind to anti-apoptotic proteins Bcl-2 and Bcl-XL to directly interact with mitochondria to promote mitochondrial membrane permeability (*13*). Additionally, the p53/p21 protein can also induce a conformational change in Bax, which triggers oligomerization and increases mitochondrial permeabilization (*33*). From the observation in this study that GE decreased the expression of p53 and p21 in the cytokine-treated cells (**Figure 9B**,**C**), it is suggested that GE inhibited apoptosis through p53 and p21 by inhibiting mitochondrial genes to enhance ROS generation. However, the effects of GE on mitochondrial membrane integrity, Bcl-2, Bcl-XL, and Bax, should be further elucidated.

We observed that GE inhibited the cleaved activation of caspase-9 in the cytokine-treated cells (**Figure 8C**). Disruption of $\Delta\psi$m results from the opening of permeability transition pores, causing a local disruption of the outer mitochondrial membrane, and leads to the release of soluble intermembrane proteins, including cytochrome *c*, and the cytochrome *c* release contributes to the activation of caspase-9 (first-level caspase; activator). It might be estimated that GE leads to the release of cytochrome *c*.

It has been reported that caspases play an essential role in β-cell death. The caspase family is a class of cysteine proteases that is involved in a cascade of protective cleavages, leading to the eventual fragmentation of DNA in mammalian cells. Of particular interest is caspase-3, the most widely studied member of the caspase family and the most important executioner of apoptosis, because it is responsible for the direct proteolytic cleavage of various cellular target proteins. Thus, caspase-3 is often used as a marker for detection of apoptosis. Activation of caspase-3 is an essential step in the execution of apoptosis, and its inhibition blocks apoptotic cell death (*34*). As demonstrated in our experiment, cytokine-induced apoptotic signaling leads to the activation of caspase-3, yet co-treatment of MIN6N8 cells with GE apparently inhibited the cleavage and activation of caspase-3. RG displayed more inhibitory effect than WG. This result indicates that ginseng exerts anti-apoptotic activity partly by preventing the apoptotic signaling that leads to the activation of caspase-3.

Our results showed that GE decreased the level of p53 and p21 in cytokine-treated cells (**Figure 9B**,**C**), suggesting that the p53/p21 pathway was regulated by GE. The p53 protein can induce apoptosis by transcriptional activation of pro-apoptotic Bcl-2 family members and repression of anti-apoptotic Bcl-2 proteins and inhibitors of pro-apoptotic proteins (*35*). In addition, p53 can also induce apoptosis in a transcriptionally independent manner. The results presented herein account for that the inhibitory effect of GE on cytokine-induced apoptosis might decrease the expression of Bax and Fas protein dependent on the p53 protein that affects mitochondrial function, raising the possibility that the expression of Bax or Fas could be transcriptionally regulated in response to GE treatment, but this issue should be elucidated.

In conclusion, our results demonstrate that GE protected cytokine-induced apoptosis in a dose-dependent manner in MIN6N8 cells. GE prevented cytokine-induced apoptosis by protection against the generation of NO and ROS, the expression of p53 and p21, and the cleaved activation of caspase-9, -3, and -7 and PARP. Therefore, we speculate that the inhibition of apoptosis observed in this study may provide a mechanism for the antidiabetic function of ginseng and that the inhibition of p53, p21, NO, ROS, cleaved caspases, and cleaved PARP may provide a mechanism for the anti-apoptotic activity of ginseng.

ABBREVIATIONS USED

IL, interleukin; IFN, interferon; TNF, tumor necrosis factor; MTT, 3-(4,5-dimethylthaizol-2-yl)-2,5-diphenyl tetrazolium bromide; NO, nitric oxide; ROS, reactive oxygen species; $\Delta\psi$m, mitochondrial transmembrane potential; JNK/SAPK, c-jun NH_2-terminal kinase/stress-activated protein kinase; PARP, poly(ADP-ribose) polymerase; DCFH-DA, 2′,7′-dichlorofuorescin diacetate; ELISA, Enzyme-Linked Immunosorbent Assay; ginsenoside Rb1, 20(*S*)-protopanaxadiol-3-[*O*-β-D-glucopyranosyl-(1→2)-β-D-glucopyranoside]-20-[*O*-β-D-glucopyranosyl(1→6)-β-D-glucopyranoside]; ginsenoside Rb2, 20(*S*)-protopanaxadiol-3-[*O*-β-D-glucopyranosyl(1→2)-β-D-glucopyranoside]-20-[*O*-α-L-arabinopyranosyl(1→6)-β-D-glucopyranoside]; ginsenoside Rc, 20(*S*)-protopanaxadiol-3-[*O*-β-D-glucopyranosyl(1→2)-β-D-glucopyranoside]-20-[*O*-α-L-arabinofuranosyl(1→6)-β-D-glucopyranoside]; ginsenoside Rd, 20(*S*)-protopanaxadiol-3-[*O*-β-D-glucopyranosyl(1→2)-β-D-glucopyranoside]-20-(*O*-β-D-glucopyranoside); ginsenoside Re, 20(*S*)-protopanaxatriol-6-[*O*-α-L-rhamnopyranosyl(1→2)-β-D-glucopyranoside]-20-(*O*-β-D-glucopyranoside); ginsenoside Rf, 20(*S*)-protopanaxatriol-6-*O*-β-D-glucopyranosyl(1→2)-β-D-glucopyranoside; ginsenoside Rg1, 20(*S*)-protopanaxatriol-6,20-di-*O*-β-D-glucoside.

LITERATURE CITED

(1) Huang, K. C. *The Pharmacology of Chinese Herbs*; CRC Press: Boca Raton, FL, 1999.

(2) Kimura, M.; Waki, I.; Chujo, T.; Kikuchi, T.; Hiyama, C.; Yamazaki, K.; Tanaka, O. Effects of hypoglycemic compounds in ginseng radix on blood insulin level in alloxan diabetic mice and on insulin release from perfused rat pancreas. *J. Pharmacobio-Dyn.* **1981**, *4*, 410−417.

(3) Kimura, M.; Waki, I.; Tanaka, O.; Nagi, Y.; Shibata, S. Pharmacological sequential trials for the fractionation of components with hypoglycemic activity in alloxan diabetic mice from ginseng radix. *J. Pharmacobio-Dyn.* **1981**, *4*, 402−409.

(4) Yokozawa, T.; Kobayashi, T.; Oura, H.; Kawashima, Y. Studies on the mechanism of the hypoglycemic activity of ginsenoside-Rb2 in streptozocin-diabetic rats. *Chem. Pharm. Bull.* **1985**, *33*, 869−872.

(5) Kimura, M.; Nakashima, N.; Sugihara, Y.; Fu-Jun, C.; Kimura, M. The antihhperglycemic blend effect of traditional Chinese medicine Byakko-ka-ninjin-to on alloxan and diabetic KK-CA^y mice. *Phytother. Res.* **1999**, *13*, 484−488.
(6) Kimura, M.; Suzuki, J. The pattern of action of blended Chinese traditional medicines to glucose tolerance curves in genetically diabetic KK-CA^y mice. *J. Pharmacobio-Dyn.* **1981**, *4*, 907−915.
(7) Chung, S. H.; Choi, C. G.; Park, S. H. Comparisons between white ginseng radix and rootlet for antidiabetic activity and mechanism in KKAy mice. *Arch. Pharmacal. Res.* **2001**, *24*, 214−218.
(8) Dey, L.; Xie, J. T.; Wang, A.; Wu, J.; Maleckar, S. A.; Yuan, C. S. Anti-hyperglycemic effects of ginseng: Comparison between root and berry. *Phytomedicine* **2003**, *10*, 600−605.
(9) Sievenpiper, J. L.; Sung, M. K.; Di Buono, M.; Leiter, L. A.; Nam, K. Y.; Vuksan, V. Korean red ginseng rootlets decrease postprandial glycemia in healthy subjects: results of an acute dose esculation study. *Diabetes* **2003**, *52 (Suppl. 1)*, A387.
(10) Sievenpiper, J. L.; Sung, M. K.; Di Buono, M.; Nam, K. Y.; Vuksan, V. Korean red ginseng rootlets decrease postprandial glycemia in healthy subjects: results from sequential batch and dose finding studies. *Proceedings of the 21st international symposium for the study of diabetes and nutrition*; June 19−21, Brugge, Belgium, 2003.
(11) Vuksan, V.; Sievenpiper, J. L.; Sung, M. K.; Di Buono, M.; Stavro, P. M.; Jenkins, A. L.; et al. Safety and efficacy of Korean red ginseng intervention (SAEKI): results of a double-blind, placebo-controlled crossover trial in type 2 diabetes. *Diabetes* **2003**, *52 (Suppl. 1)*, A137.
(12) Cnop, M.; Welsh, N.; Jonas, J. C.; Jorns, A.; Lenzen, S.; Eizirik, D. L. Mechanisms of pancreatic β-cell death in type 1 and type 2 diabetes. *Diabetes* **2005**, *54*, S97−S107.
(13) Kim, W. H.; Lee, J. W.; Gao, B.; Jung, M. H. Synergistic activation of JNK/SAPK induced by TNF-α and IFN-γ: Apoptosis of pancreatic β-cells via the p53 and ROS pathway. *Cell. Signalling* **2005**, *17*, 1516−1532.
(14) Attele, A. S.; Wu, J. A.; Yuan, C. S. Multiple pharmacological effects of ginseng. *Biochem. Pharmacol.* **1999**, *58*, 1685−1693.
(15) Lau, A. J.; Woo, S. O.; Koh, H. L. Analysis of saponins in raw and steamed Panax notoginseng using high-performance liquid chromatography with diode array detection. *J. Chromatogr., A* **2003**, *1011*, 77−87.
(16) Yagi, N.; Yokono, K.; Amano, K.; Nagata, M.; Tsukamoto, K.; Hasegawa, Y.; Yoneda, R.; Okamoto, N.; Moriyama, H.; Miki, M.; Tominaga, Y.; Miyazaki, J. I.; Yagita, H.; Okumura, K.; Mizoguchi, A.; Miki, A.; Ide, C.; Maeda, S.; Kasuga, M. Expression of intercellular adhesion molecule 1 on pancreatic β-cell destruction by cytotoxic T-cells in murine autoimmune diabetes. *Diabetes* **1995**, *44*, 744−752.
(17) Di Matteo, M. A.; Loweth, A. C.; Thomas, S.; Mabley, J. G.; Morgan, N. G.; Thorpe, J. R.; Green, I. C. Superoxide, nitric oxide, peroxynitrite and cytokine combinations all cause functional impairment and morphological changes in rat islets of langerhans and insulin-secreting cell lines but dictate cell death by different mechanism. *Apoptosis* **1997**, *2*, 164−177.
(18) Kumar, R.; Mandal, M.; Lipton, A.; et al. Overexpression of HER2 modulate BCL-2, BCL-XL and tamoxifen-induced apoptosis in human MCF-7 breast cancer cells. *Clin. Cancer Res.* **1996**, *2*, 1215−1219.
(19) Green, L. C.; Wagner, D. A.; Glogowski, J.; Skipper, P. L.; Wishnok, J. S.; Tannerbaum, S. R. Analysis of nitrate, nitrite, and [15N]nitrate in biological fluids. *Anal. Biochem.* **1982**, *126*, 131−138.
(20) Takeshi, N.; Diane, E.; Xue, L. D.; Sho, I. Y.; Takeshi, M.; Yasufumi, K.; Mark, A. Y.; David, B.; Peter, J. O.; Hans, P. H.; Ida, G.; Michael, B. Normalizing mitochondrial superoxide production blocks three pathways of hyperglycemic damage. *Nature* **2000**, *404*, 787−790.
(21) Allen, R. T.; Hunter, W. J., III; Agrawal, D. W. Morphological and biochemical characterization and analysis of apoptosis. *J. Pharmacol. Toxicol.* **1997**, *37*, 215−228.
(22) Moncada, S.; Palmer, R. M.; Higgs, E. A. Nitric oxide: physiology, pathophysiology, and pharmacology. *Pharmacol. Rev.* **1991**, *43*, 109−142.
(23) Chang, I.; Cho, N.; Kim, S.; Kim, J. Y.; Kim, E.; Woo, J.; Nam, J. H.; Kim, S. J.; Lee, M. S. Role of calcium in pancreatic islet cell death by IFN-γ/TNF-α. *J. Immunol.* **2004**, 7008−7014.
(24) Levine, A. J. p53, the cellular gatekeeper for growth and division. *Cell* **1997**, *88*, 32f3−331.
(25) Tewari, M.; Quan, L. T.; O'Rourke, K.; Desnoyers, S.; Zeng, Z.; Beidler, D. R.; Poirier, G. G.; Salvessen, G. S.; Dixit, V. M. Yama/CPP32β, a mammalian homology of CED-3, is a CrmA-inhibitable protease that cleaves the death substrate poly(ADP-ribose) polymerase. *Cell* **1995**, *81*, 801−809.
(26) Ankarcrona, M.; Dypbukt, J. M.; Brune, B.; Nicotera, P. Interleukin-1 beta-induced nitric oxide production activates apoptosis in pancreatic RINm5F cells. *Exp. Cell Exp.* **1994**, *213*, 172−177.
(27) Mandrup-Poulsen, T. The role of interleukin-1 in the pathogenensis of IDDM. *Diabetologia* **1996**, *39*, 1005−1029.
(28) Messmer, U. K.; Ankarcrona, M.; Nicotera, P.; Brune, B. p53 expression in nitric oxide-induced apoptosis. *FEBS Lett.* **1994**, *355*, 23−26.
(29) Rabinovitch, A.; Suarez-Pinzon, W. L.; Strynadka, K.; Lakey, J. R.; Rajott, R. V. Human pancreatic islet β-cell destruction by cytokines involves oxygen free radical and aldehyde production. *J. Clin. Endocrinol. Metab.* **1996**, *81*, 3197−3202.
(30) Green, D. R.; Reed, J. C. Mitochondria and apoptosis. *Science* **1998**, *281*, 1309−1312.
(31) Sansome, C.; Zaika, A.; Marchenko, N. D.; Moll, U. T. Hypoxia death stimulus induces translocation of p53 protein to mitochondria. *FEBS Lett.* **2001**, *488*, 110−115.
(32) Li, P.-F.; Dietz, R.; Harsdorf, R. p53 regulates mitochondrial membrane potential through reactive oxygen species and induces cytochrome *c*-independent apoptosis blocked by Bcl-2. *EMBO J.* **1999**, *18*, 6027−6036.
(33) Cheng, E. H.; Wei, M. C.; Weiler, S. W.; Flavell, R. A.; Mak, T. W.; Lindsten, T.; Korsmeyer, S. J. Bcl-2, Bcl-XL sequester BH3 domain-only molecules preventing BAX- and BAK-mediated mitochondria apoptosis. *Mol. Cell* **2001**, *8*, 705−711.
(34) Mathis, D.; Vence, L.; Benoist, C. β-cell death during progression to diabetes. *Nature* **2001**, *414*, 792−798.
(35) Donath, M. Y.; Gross, D. J.; Cerasi, E.; Kaiser, N. Hyperglycemia-induced β-cell apoptosis in pancreatic islets of *Psammomys obesus* during development of diabetes. *Diabetes* **1999**, *48*, 738−744.

Received for review September 7, 2006. Revised manuscript received February 16, 2007. Accepted February 21, 2007. This work was supported by Korea Food Research Institute (Grants E066006 and E070802).

JF062577R